Pis'ma v ZhETF, vol. 92, iss. 4, pp. 242 – 250 © 2010 August 25

Compensation temperatures, magnetic susceptibilities and phase diagrams of a mixed ferrimagnetic ternary system on the Bethe lattice

B. Deviren[+*], *M. Keskin*[∇1)], *Y. Aydın*[□]

[+]*Institute of Science, Erciyes University, 38039 Kayseri, Turkey*

[*]*Department of Physics, Nevşehir University, 50300 Nevşehir, Turkey*

[∇]*Department of Physics, Erciyes University, 38039 Kayseri, Turkey*

[□]*Institute of Science, Nevşehir University, 50300 Nevşehir, Turkey*

Submitted 11 May 2010

Compensation behaviors, magnetic susceptibilities and the phase diagrams of the ternary system of the type ABC consisting of Ising spins $\sigma = 1/2$, $S = 3/2$ and $m = 5/2$ in the presence of a single-ion anisotropy are studied on the Bethe lattice within the framework of the exact recursion relations. Both ferromagnetic and antiferromagnetic exchange interactions are considered. The exact expressions for sublattice magnetizations and magnetic susceptibilities are obtained, and then thermal behaviors of the sublattice magnetizations, total magnetization, magnetic sublattice susceptibilities and total susceptibility are investigated. We find that the system only undergoes a second order phase transition for the different and same bilinear nearest-neighbor exchange interaction parameters, but displays compensation behaviors for only different bilinear interaction parameters. We also present the phase diagrams for the different and same bilinear nearest-neighbor exchange interaction parameters. A comparison is made with the other ternary system of the type ABC consisting of different spin values.

During the last two decades, the ternary system ABC corresponding to the Prussian blue analogs, which are the prime examples of molecular-based magnets, has been intensively studied experimentally and theoretically (see [1 – 3] and references therein). These materials have interesting magnetic properties such as the photoinduced magnetization effect [4], the tuning of the color of magnetic thin film [5, 6], inverting magnetic hysteresis loop [7], a charge-transfer-induced spin transitions [8 – 10], and hydrogen storage capacity [11]. These materials may also exhibit compensation temperatures where the total magnetization vanishes below the critical temperature. The existence of compensation temperatures is of great technological importance since at this point only a small driving field is required to change the sign of the total magnetization. This property is very useful in thermomagnetic recording, electronic and computer technologies [12, 13]. Many more experimental works have been done about Prussian blue analogs (see [14 – 18] and references therein). On the other hand, the ternary alloy AB_pC_{1-p} composed of Prussian blue analogs has been also studied theoretically. For example, the magnetic properties of a mixed ferro-ferrimagnetic ternary system of the type ABC consisting of Ising spins 1/2, 1, 3/2 were studied by the use of a mean-field theory (MFT) based on Bogoliubov inequality for the Gibbs free energy [19] and the effective-field theory (EFT) [20, 21]. Recently, the critical behavior of this mixed ternary system were also investigated on the Bethe lattice by using the exact recursion relations for the same [22] and different [23] bilinear nearest-neighbor exchange interaction parameters. The magnetic properties of the ternary system consisting of spins 1, 3/2, 5/2 were studied within the MFT [24], the MFT based on Bogoliubov inequality for the Gibbs free energy [25 – 27], the EFT [28] and the Monte Carlo (MC) simulation [29]. The ground-state phase diagrams of the AB_pC_{1-p} ternary alloy cons isting of Ising spins 3/2, 1, and 5/2 in the presence of single-ion anisotropy have also constructed [30]. The mixed ferro-ferrimagnetic ternary system with Ising spins 1/2, 1, 5/2 was used to study the spin fluctuation effect on the appearance of plural compensation temperatures by the combination of molecular-field approximation, decorated-iteration transformation and the MC simulation [31]. The magnetic properties (phase diagram, magnetization, compensation temperature, and magnetic susceptibility) of the AB_pC_{1-p} ternary alloy consisting of spins 3/2, 2, 5/2 were investigated by the use of the MFT based on Bogoliubov inequality for the Gibbs free energy [32-34] and the MC simulations [35].

Thus, although considerable progress has been made in understanding the magnetic properties of the ABC

[1)]e-mail: keskin@erciyes.edu.tr

ternary system consisting of half-integer and integer spin variables, only one work about the magnetic properties of the ternary system with only the half-integer spin variables, best of our knowledge, only one work has been studied on an anisotropically decorated square lattice by Čanová et. al [36]. In this paper, we are going to study compensation temperatures, magnetic susceptibilities and the phase diagrams of the ternary system of the type ABC consisting of consisting of only half-integer Ising spins, namely σ=1/2, $S = 3/2$ and $m = 5/2$, in the presence of a single-ion anisotropy on the Bethe lattice within the framework of the exact recursion relations. Both ferromagnetic and antiferromagnetic exchange interactions are considered. The exact expressions for the sublattice magnetizations and magnetic susceptibilities are obtained, and thermal behaviors of the sublattice magnetizations, total magnetization, magnetic sublattice susceptibilities and total susceptibility are investigated. We also present the phase diagrams including the compensation behaviors for different and same bilinear interaction parameters. We find that this system exhibits very different magnetic properties as would be seen in the upcoming sections. Finally, it is worthwhile mentioning that it is now widely recognize that in many cases solutions of spin systems on Bethe or generalized Bethe lattices are qualitatively better approximations for the regular lattices than the solutions obtained by conventional mean-field theories, because of the presence of correlations in the former and the lack of correlations in the latter [37]. One should also mention that the Bethe lattice consideration has some limitations, such as it predicts a higher transition temperature than a regular lattice and it is not reliable for predicting critical exponents [37].

The Hamiltonian for the mixed Ising model of the type ABC ternary system consisting of half-integer spins $\sigma = 1/2$, $S = 3/2$ and $m = 5/2$ on the Bethe lattice is given by

$$H = -J_1 \sum_{\langle ij \rangle} \sigma_i S_j - J_2 \sum_{\langle jk \rangle} S_j m_k - \\ - J_3 \sum_{\langle ik \rangle} \sigma_i m_k + \Delta \left(\sum_j S_j^2 + \sum_k m_k^2 \right) - \\ - h \left(\sum_i \sigma_i + \sum_j S_j + \sum_k m_k \right), \quad (1)$$

where each σ_i,S_j and m_k located at the sites i, j and k are a spin-1/2 with the two discrete values $\pm 1/2$, a spin-3/2 with the four discrete values $\pm 3/2$ and $\pm 1/2$, and a spin-5/2 with the six discrete values $\pm 5/2$, $\pm 3/2$ and $\pm 1/2$, respectively. J_1, J_2 and J_3 are the bilinear nearest-neighbor exchange interactions and we consider both ferromagnetic (J_3>0) and antiferromagnetic (J_2<0) and (J_1<0) exchange interactions. Δ and h are the single-ion anisotropy and external magnetic field, respectively. The first three summations are performed for nearest-neighbor (NN) spin pairs, the last sums run over all the spin-3/2 and spin-5/2 sites. In this ternary system case, we arrange the Bethe lattice such that the central spin is spin-1/2, σ_0; the second generation is spin-3/2, S_0; the third generation is a spin-5/2, m_0; the fourth generation is again spin-1/2, σ_1; the fifth generation is again spin-3/2, S_1; the sixth generation is again spin-5/2, m_1; so on to infinity, as seen in Fig.1 for q = 3, respectively. It is seen from the Fig.1 that the central spin has q NN, i.e., the coordination number, which forms the second generation spins. Each spin in the second generation is joined to (q-1) NN's; hence, in total, the second generation has q(q-1) NN spins that forms the third generation spins and so on to infinity.

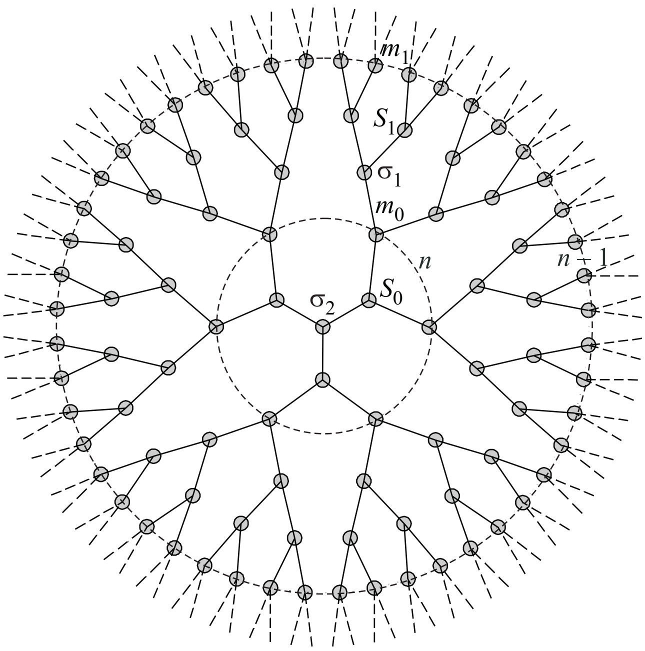

Fig.1. Bethe lattice, or regular tree, of coordination numbers ($q = 3$) for the ternary system consisting of spins $\sigma = 1/2$, $S = 3/2$, and $m = 5/2$. The Bethe lattice is arranged such that the central spin is spin-1/2, σ_0; the second generation is spin-3/2, S_0; the third generation is a spin-5/2, m_0; the fourth generation is again spin-1/2, σ_1; the fifth generation is again spin-3/2, S_1; the sixth generation is again spin-5/2, m_1; so on to infinity

The partition function is the main ingredient to obtain a formulation in terms of the recursion relations. Using the definition, the partition function of the system is given by

$$Z = \sum_{\{\sigma,\,S,\,m\}} \exp\,[-\beta\,H] =$$
$$= \sum_{\{\sigma,\,S,\,m\}} \exp\left[\beta\left(J_1 \sum_{\langle ij\rangle} \sigma_i S_j + \right.\right.$$
$$\left.\left. + J_2 \sum_{\langle jk\rangle} S_j m_k + J_3 \sum_{\langle ik\rangle} \sigma_i m_k\right)\right] +$$
$$+ \sum_{\{\sigma,\,S,\,m\}} \exp\left[-\beta\,\Delta\left(\sum_j S_j^2 + \sum_k m_k^2\right)\right] +$$
$$+ \sum_{\{\sigma,\,S,\,m\}} \exp\left[\beta\,h\left(\sum_i \sigma_i + \sum_j S_j + \sum_k m_k\right)\right], \quad (2)$$

where the summation is over all spin sets. If we cut the Bethe lattice in some central point deep inside with a spin σ_0, that is a spin-1/2, it splits up to q identical branches in which each of these branches is a rooted tree at the central spin σ_0. Therefore, the partition function for the central site on the Bethe lattice can be written as

$$Z = \sum_{\{\sigma_0\}} \exp\,[\beta h\,\sigma_0] \times [g_n\,(\sigma_0|S_0, m_0)]^q\,, \quad (3)$$

where σ_0 is the central spin value on the lattice, and is the partition function of an individual branch and the suffix n represents the fact that the sub-tree has n-shells, i.e., n steps from the root to the boundary sites. Each branch can be cut on the site which is the nearest to the central point. Therefore, is written in terms of the summation over spin set as

$$g_n\,(\sigma_0|S_0, m_0) =$$
$$= \sum_{\{S_0\}} \exp\left[\beta\left(J_1\,\sigma_0 S_0 - \Delta S_0^2 + h\,S_0\right)\right] \times$$
$$\times\,[g_n\,(S_0|m_0, \sigma_1)]^{q-1}\,. \quad (4)$$

Advancing along the any branch, we get a site that next-nearest to the central spin, hence $g_n(S_0|m_0,\sigma_1)$ is expressed as follows

$$g_n\,(S_0|m_0, \sigma_1) =$$
$$= \sum_{\{m_0\}} \exp\left[\beta\left(J_2\,S_0 m_0 - \Delta m_0^2 + h\,m_0\right)\right] \times$$
$$\times\,[g_n\,(m_0|\sigma_1, S_1)]^{q-1}\,, \quad (5)$$

We will continue until we reach a recursive point and terminate the calculation of $g_n$function.

Therefore, $g_n\,(m_0|\sigma_1, S_1)$ can be written as

$$g_n\,(m_0|\sigma_1, S_1) =$$
$$= \sum_{\{\sigma_1\}} \exp\left[\beta\left(J_3\,m_0\sigma_1 - \Delta\sigma_1^2 + h\,\sigma_1\right)\right] \times$$
$$\times\,[g_{n-1}(\sigma_1|S_1, m_1)]^{q-1}\,, \quad (6)$$

where is the partition function of the next shell, i.e., the (n-*1*)th shell, seen in Fig.1. Therefore, in this way, the expression for in the nth-shell is obtained in terms of in the (n-*1*)th shell. As seen from Fig.1, these shells are identical.

In order to find the exact recursion relations, we introduce the following variables as a ratio of the gn function for the spin-1/2:

$$N_n = \frac{g_n(1/2)}{g_n(-1/2)}, \quad (7)$$

for the spin-3/2:

$$X_n = \frac{g_n(3/2)}{g_n(-1/2)},\ Y_n = \frac{g_n(-3/2)}{g_n(-1/2)},\ Z_n = \frac{g_n(1/2)}{g_n(-1/2)}, \quad (8)$$

and for the spin-5/2:

$$A_n = \frac{g_n(5/2)}{g_n(-1/2)},\ B_n = \frac{g_n(-5/2)}{g_n(-1/2)},\ C_n = \frac{g_n(3/2)}{g_n(-1/2)},$$

$$D_n = \frac{g_n(-3/2)}{g_n(-1/2)},\ E_n = \frac{g_n(1/2)}{g_n(-1/2)}, \quad (9)$$

The variables N_n, X_n, Y_n, Z_n, A_n, B_n, C_n, D_n and E_n can obtain by using Eqs. (4)-(6) and these explicit expressions are given in Appendix. We should mention that these recursion relations have no direct physical sense, but all thermodynamic functions can be obtained from these relations and they reflect the critical behavior of the system. Thus, we can say that in the thermodynamic limit ($n \longrightarrow \infty$), the above-mentioned variables determine the status of the system.

Now we can calculate the sublattice magnetizations for spins 1/2, 3/2 and 5/2. If the central spin is chosen to be a spin-1/2 (σ_0), the first sublattice magnetization of the system is defined by

$$M_{1/2} = Z^{-1} \sum_{\{\sigma_0\}} \sigma_0\,[g_n(\sigma_0|S_0, m_0)]^q\,, \quad (10)$$

which is easily expressed in terms of the recursion relations, namely Eqs. (7)-(9), and calculated as

$$M_{1/2} = \frac{e^{\beta(-\Delta/4+h/2)}\,N_n^q - e^{\beta\,(-\Delta/4\,-\,h/2)}}{2\,e^{\beta\,(-\Delta/4+h/2)}\,N_n^q + 2\,e^{\beta\,(-\Delta/4\,-\,h/2)}}. \quad (11)$$

The next step is to calculate the sublattice magnetization $M_{3/2}$ for a spin-3/2. We can again start from the first shell on the Bethe lattice, and carry out the whole calculation by choosing the spin-3/2 (S_0) as the central-spin instead of spin-1/2 (σ_0), since all sites with the same kinds of spins are equivalent deep inside the Bethe lattice. We perform similar calculation, and rearranging it for the spin-3/2's as we have done for $\sigma = 1/2$, we find

$$M_{3/2} = \frac{\left\{\begin{array}{l} 3\, e^{\beta(-9\Delta/4+3h/2)}\, X_n^q - 3\, e^{\beta(-9\Delta/4-3h/2)}\, Y_n^q \\ +e^{\beta(-\Delta/4+h/2)}\, Z_n^q - e^{\beta(-\Delta/4-h/2)} \end{array}\right\}}{\left\{\begin{array}{l} 2\, e^{\beta(-9\Delta/4+3h/2)}\, X_n^q + 2\, e^{\beta(-9\Delta/4-3h/2)}\, Y_n^q \\ +2\, e^{\beta(-\Delta/4+h/2)}\, Z_n^q + 2\, e^{\beta(-\Delta/4-h/2)} \end{array}\right\}}. \tag{12}$$

Finally, if the central-spin is chosen a spin-5/2 (m_0), we obtain the third sublattice magnetization with the similar calculation as above

$$M_{5/2} = \frac{\left\{\begin{array}{l} 5\, e^{\beta(-25\Delta/4+5h/2)}\, A_n^q - 5\, e^{\beta(-25\Delta/4-5h/2)}\, B_n^q \\ +3\, e^{\beta(-9\Delta/4+3h/2)}\, C_n^q - 3\, e^{\beta(-9\Delta/4-3h/2)}\, D_n^q \\ +e^{\beta(-\Delta/4+h/2)}\, E_n^q - e^{\beta(-\Delta/4-h/2)} \end{array}\right\}}{\left\{\begin{array}{l} 2\, e^{\beta(-25\Delta/4+5h/2)}\, A_n^q + 2\, e^{\beta(-25\Delta/4-5h/2)}\, B_n^q \\ +2\, e^{\beta(-9\Delta/4+3h/2)}\, C_n^q + 2\, e^{\beta(-9\Delta/4-3h/2)}\, D_n^q \\ +2\, e^{\beta(-\Delta/4+h/2)}\, E_n^q + 2 e^{\beta(-\Delta/4-h/2)} \end{array}\right\}}. \tag{13}$$

In order to determine the compensation temperature T_{Comp} at which the total magnetization vanishes below the critical temperature, one has to calculate the total magnetization. The total magnetization per site is defined as

$$M_{\mathrm{T}} = M_{1/2} + M_{3/2} + M_{5/2}. \tag{14}$$

It is worthwhile mentioning that the occurrence of a compensation point is due to the fact that the magnetic moments of sublattices compensate each other completely at $T = T_{\mathrm{Comp}}$ owing to different temperature dependences of the sublattice magnetizations. The existence of a compensation temperature near the room temperature in some ferrrimagnetic materials has a crucial importance in the area of the thermomagnetic recording devices, electronic and computer technologies [12, 13]. Moreover, it has been found that some physical properties show a peculiar behavior at this point. For example, the coercivity field is strongly temperature dependent only in the proximity of the compensation temperature in which it is a maximum at T_{Comp}, falling to minimum below T_{Comp}, before rising again at low temperatures [39–41].

Thus, we found the sublattice and total magnetizations in terms of the recursion relations. All information about the behavior of the system can be obtained from these equations, namely Eqs. (11)–(14). For example, we can easily calculate the magnetic susceptibilities in which give some important physical properties of the system for spins-1/2, 3/2 and 5/2 by using the Eqs. (11)-(13). The susceptibility for the system can be determined easily from the following equation:

$$\chi_\alpha = \lim_{h\to 0} \frac{\partial M_\alpha}{\partial h}, \tag{15}$$

where $\alpha = 1/2$, 3/2 and 5/2 is taken the values of the sublattice magnetizations. Hence, total susceptibility is given by

$$\chi_{Total} = \chi_{1/2} + \chi_{3/2} + \chi_{5/2} = \\ = \lim_{h\to 0} \frac{\partial M_{1/2}}{\partial h} + \lim_{h\to 0} \frac{\partial M_{3/2}}{\partial h} + \lim_{h\to 0} \frac{\partial M_{5/2}}{\partial h}. \tag{16}$$

We first investigate the behaviors of sublattice magnetizations and total magnetization as well as susceptibilities as a function of the temperature for various values of the bilinear interactions and the single-ion anisotropy, and the coordination number, $q = 6$. Thermal behaviors of sublatice magnetizations are obtained solving Eqs. (11)-(13) by using iterations in the recursion relations. Thermal variation of the total magnetization is found by using Eq. (14). Moreover, temperature dependence of the sublattice and total susceptibilities is examined by solving Eqs. (15) and (16) using iterations in the recursion relations, respectively. A few interesting results are plotted in Figs.2 and 5 in order to illustrate the calculation of the phase transition points as well as obtain the compensation temperatures and their type of behaviors.

From Fig.2, we have seen that the system always undergoes a second-order phase transition, because sublattice magnetizations become zero continuously as the temperature increases, i.e., discontinuity does not occur for the sublattice magnetizations. One can see that the behaviors of the sublattice magnetizations in Figs. 2a-d are the similar behavior, except at the absolute zero temperature $\sigma = 1/2$, S = -3/2, $m = 5/2$ in Fig.2a; $\sigma = 1/2$, S = -3/2, $m = 3/2$ in Fig.2a, $\sigma = 1/2$, S = -3/2, $m = 1/2$ in Fig.2c and $\sigma = 1/2$, S = -1/2, $m = 1/2$ in Figs.2d. On the other hand, we have found that the system always exhibits the compensation behaviors and their type either the N-type, seen in Figs. 2a, b and d or the P-type, shown in Fig.2c, in the Neel classification nomenclature [42, 43]. We have studied the thermal behavior of the sublattice magnetizations and the total magnetization for different coordination numbers, q, and found that when q is large the critical and compensation temperatures

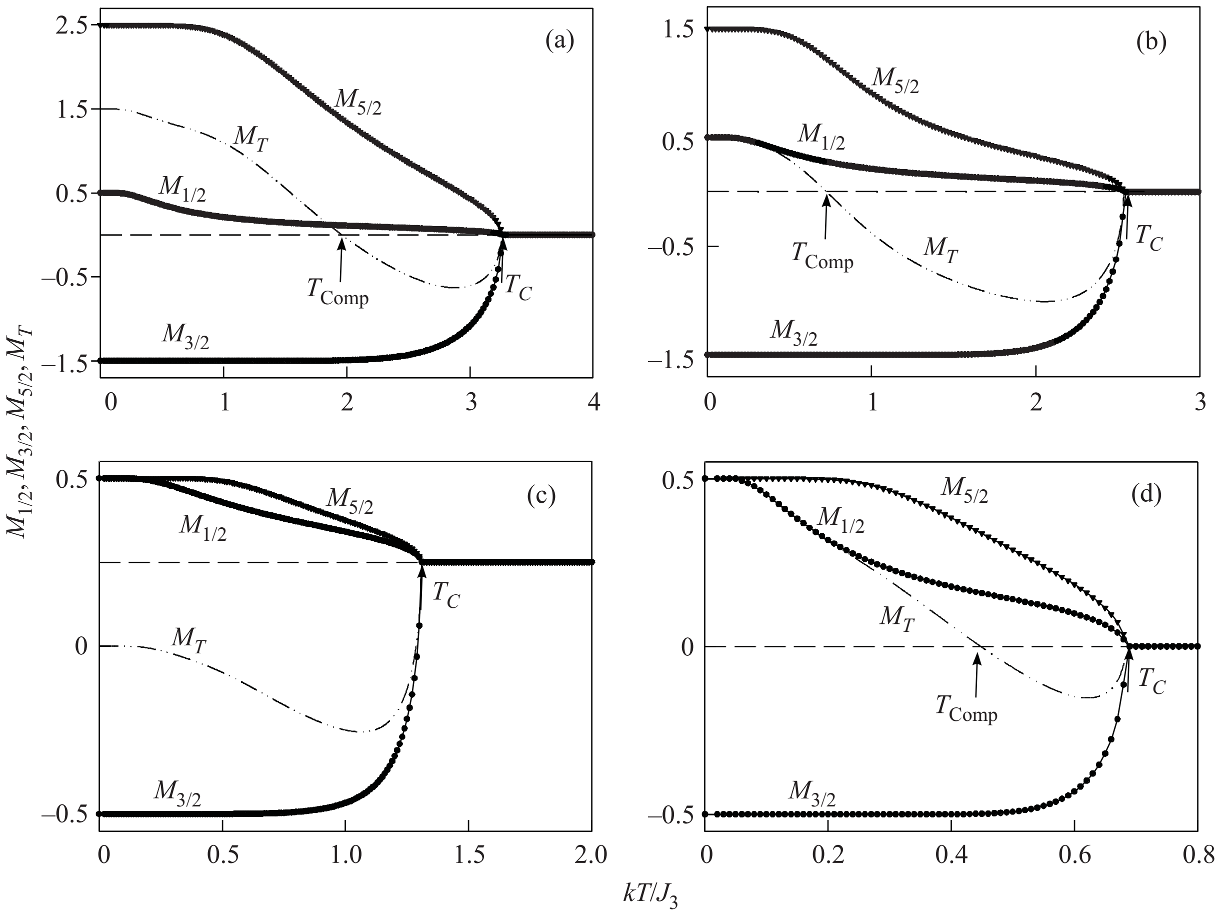

Fig.2. (a) Temperature dependence of sublattice and total magnetizations for $J_1 = -0.1$, $J_2 = -2.0$, $J_3 = 1.0$ with $q = 6$, T_C and $T_{\rm Comp}$ are the second-order phase transition or critical temperature and the compensation temperature respectively. **(a)** $\Delta/J_3 = -1.5$, (b) $\Delta/J_3 = 1.0$, (c) $\Delta/J_3 = 2.5$, (d) $\Delta/J_3 = 5.0$

occur for high temperature values, otherwise occur low temperature values. We have also examined the thermal behavior of the sublattice magnetizations and total magnetization for the same value of bilinear nearest-neighbor exchange interaction parameters and found that the system for the same bilinear nearest-neighbor interactions always undergoes a second-order phase transition, but does not exhibit the compensation behaviors.

Fig.3 illustrate the thermal behaviors of the sublattice magnetizations and susceptibilities χ_α ($\alpha = 1/2$, $3/2$, $5/2$) for $J_1 = -0.1$, $J_2 = -2.0$, $J_3 = 1.0$ and $\Delta/J_3 = -1.5$ with $q = 6$. In Fig.3a, $\sigma = 1/2$, $S = -3/2$, $m = 5/2$ at zero temperature and σ and m decrease and S increases to the zero value continuously as the temperature increases, therefore a second-order phase transition occurs $T_C = 3.275$ and the phase transition is from the ferrimegnetic phase of (1/2, -3/2, 5/2) to the paramagnetic phase. In Fig.3b, when the temperature approaches to T_C, the $\chi_{1/2}$ and $\chi_{5/2}$ sublattice susceptibilities increase very rapidly and go to positive infinity at T_C. On the other hand, the $\chi_{3/2}$ sublattice susceptibility decreases very rapidly and goes to negative infinity at T_C. It is also seen from this figure that the susceptibilities $\chi_{1/2}$ and $\chi_{5/2}$ exhibit the usual temperature variation in the vicinity of T_C, but the $\chi_{3/2}$ sublattice susceptibility take negative values. We note that, in general, $\chi_{1/2}$ and $\chi_{5/2} \longrightarrow +\infty$, and $\chi_{3/2} \longrightarrow$ $-\infty$ as $T \longrightarrow T_C$ if in the vicinity of T_C the following relation of the magnitude among sublattice magnetizations is satisfied: $|M_{1/2}|+ |M_{3/2}|> |M_{5/2}|$. We have found similar susceptibilities behavior to the one seen in the magnetic properties of a mixed ferro-ferrimagnetic ternary systems of spins 1/2, 1, 3/2 [20, 22, 23]. The total susceptibility has the similar behavior of $\chi_{3/2}$.

We also investigate the behaviors of the sublattice magnetizations, the total magnetization, and magnetic sublattice susceptibilities as a function of the single-ion anisotropy and present one representative graph for J_1 = -0.1, J_2 = -2.0, J_3 = 1.0 and kT/J_3 = 0.05 with $q = 6$, seen in Fig.4. Figs.4a and b display one of the more in-

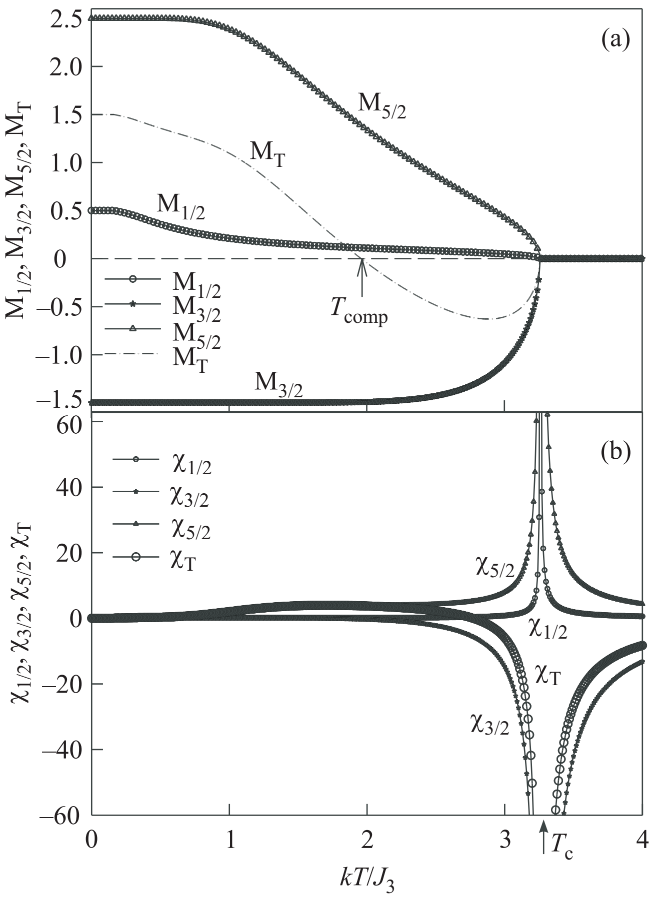

Fig.3.(a) Temperature dependence of sublattice and total magnetizations for $J_1 = -0.1$, $J_2 = -2.0$, $J_3 = -1.0$, $\Delta/J_3 = -1.5$ with $q = 6$, T_C and T_{Comp} are the second-order phase transition or critical temperature and the compensation temperature, respectively. (b) Temperature dependence of magnetic sublattice and total susceptibilities for $J_1 = -0.1$, $J_2 = -2.0$, $J_3 = -1.0$, $\Delta/J_3 = -1.5$ with $q = 6$

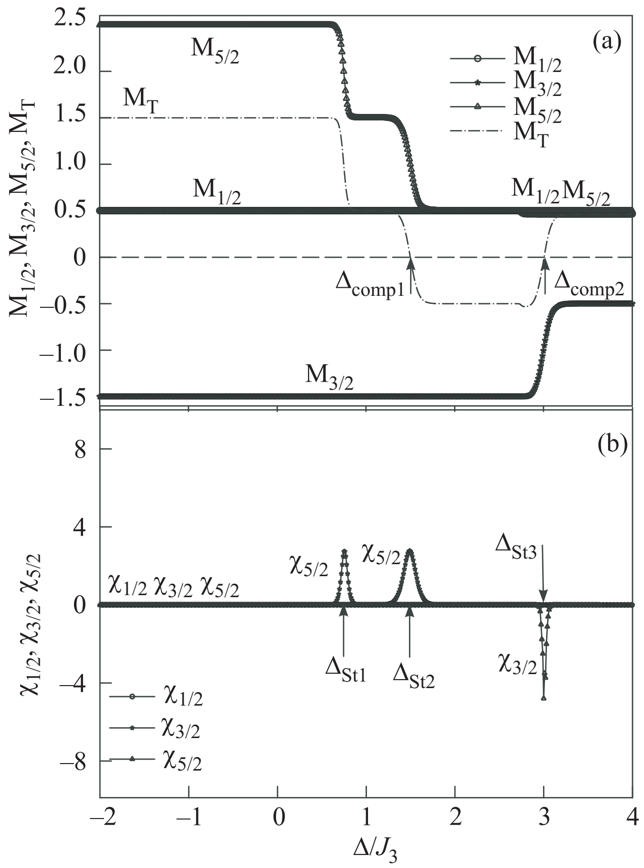

Fig.4. The behavior of magnetizations and magnetic susceptibilities as a function of the single-ion anisotropy for $J_1 = -0.1$, $J_2 = -2.0$, $J_3 = 1.0$ and $kT/J_3 = 0.05$ with $q = 6$. Δ_C, Δ_{Comp} and $\Delta_{\text{St}\,i}$ are the second-order phase transition, the compensation effect start and finish values, and the separation point, respectively. (a) For the sublattice and total magnetizations. (b) For the susceptibilities

teresting behavior of the system as follows. At very low values of the single-ion anisotropy Δ/J_3 we have $M_{1/2} = 1/2$, $M_{3/2}$ = -3/2 and $M_{5/2}$ = 5/2; hence the system exists the ferrimagnetic phase of (1/2, -3/2, 5/2), as the reduced single-ion anisotropy (Δ/J_3) increases the ferrimagnetic phase of (1/2, -3/2, 5/2) smoothly passes to the ferrimagnetic phase of (1/2, -3/2, 3/2) without any phase transition, and as the values of Δ/J_3 increases further the ferrimagnetic phase of (1/2, -3/2, 3/2) smoothly passes to the ferrimagnetic phase of (1/2, -3/2, 1/2) without any phase transition (marked as Δ_{St1} and Δ_{St2} that are called staggered points). Moreover, when the values of Δ/J_3 increases further the ferrimagnetic phase of (1/2, -3/2, 1/2) smoothly passes to the ferrimagnetic phase of (1/2, -1/2, 1/2) without any phase transition (one more staggered point which marked as Δ_{St3}. One can analyze the situation as follows. For a half-integer sublattice, if the single-ion anisotropy is negative and large enough, all the spins on B and C sublattices will be at the spin-1/2 phase instead of the spin-3/2 and spin-5/2 phases, respectively, at ground state; hence the system becomes the ferrimagnetic (1/2, -1/2, 1/2) phase. Actually, when moving along the vertical axis in the up-down direction, the single-ion anisotropy parameter Δ/J_3 forces the central spins to their lower spin state. Thus, a smooth passing, with no phase transition singularity, can occur between these phases. We have found a similar behavior to the one seen in the phase diagrams of the two-su blattice spin-3/2 Ising model by using the renormalization group calculation [44], mixed ternary system of spins $\sigma = 1/2$, $S = 1$ and $m = 3/2$ on the Bethe lattice [22, 23] and also in the mixed spin-1/2 and spin-5/2 Ising system within the effective-field theory [45]. We should also mention that the peaks or maxima for the susceptibilities of spin-5/2, marked with Δ_{St1} and Δ_{St2}, and for the susceptibilities of spin-3/2, marked with Δ_{St3} are the separation points of these ordered phases, seen in Fig.4b.

We can now present the phase diagrams including the compensation temperatures. The calculated phase diagrams are presented in the $(kT/J_3,\ \Delta/J_3)$ plane for the different values of bilinear nearest-neighbor exchange interaction parameters, seen in Fig.5 for $q = 6$. In these phase diagrams, the solid line represents the second-order phase transition line and the dashed-dot-dot lines illustrate the compensation temperatures. For very low values of the reduced single-ion anisotropy Δ/J_3 we have the (1/2, -3/2, 5/2) ferrimagnetic phase. When the value of the Δ/J_3 increases, the system sequentially passes to the (1/2, -3/2, 3/2), (1/2, -3/2, 1/2), and (1/2, -1/2, 1/2) ferromagnetic phases without any phase transition.

We also calculate the phase diagram of the system in the (kT/J_3), Δ/J_3 plane for the same values of the bilinear nearest-neighbor exchange interaction parameters, namely $J_1 = J_2 = J_3 = 1.0$, seen in Fig.6 for $q = 3$ and 6. From Fig.6, one can see that the system always undergoes a second-order phase transition; hence the tricritical behavior does not exist. For very low values of the reduced single-ion anisotropy the (1/2, 3/2, 5/2) ferrimagnetic phase exists, but for high values of the reduced single-ion anisotropy and the low reduced temperature, the (1/2, 1/2, 1/2) ferromagnetic phase exists.

In conclusion, the ternary system of the type ABC consisting of Ising spins $\sigma = 1/2$, $S = 3/2$ and $m = 5/2$ in the presence of a single-ion anisotropy for the different values of bilinear nearest-neighbor exchange interaction parameters on the Bethe lattice exhibits the compensation behavior to the one seen in the ABC ternary system composed of half-integer and integer spin variables, namely spins 1/2, 1, 3/2 [20, 23], with Ising spins 3/2, 5/2, 3/2 [24], with Ising spins 1, 3/2, 5/2 [26, 28, 29] and with Ising spins 3/2, 2, 5/2 [33–35]. The present system only undergoes a second order phase transition; hence it does not exhibit the tricritical behavior. However, the ABC ternary system composed of half-integer and integer spin variables, namely spins 1/2, 1, 3/2 [19, 22, 23], with Ising spins 1, 3/2, 5/2 [25, 27] and with Ising spins 3/2, 2, 5/2 [33] display the tricritical behavior; hence these systems undergo both second- and first-order phase transitions. The present system for the same values of bilinear nearest-neighbor exchange interaction parameters on the Bethe lattice also always undergoes a second-order phase transition, but the ternary system of Ising spins 1/2, 1, 3/2 for the same values of bilinear nearest-neighbor exchange interaction parameters on the Bethe lattice undergoes a second-order phase transition for $q \leq 3$, a second- and first-order phase transition for $q > 3$ [23].

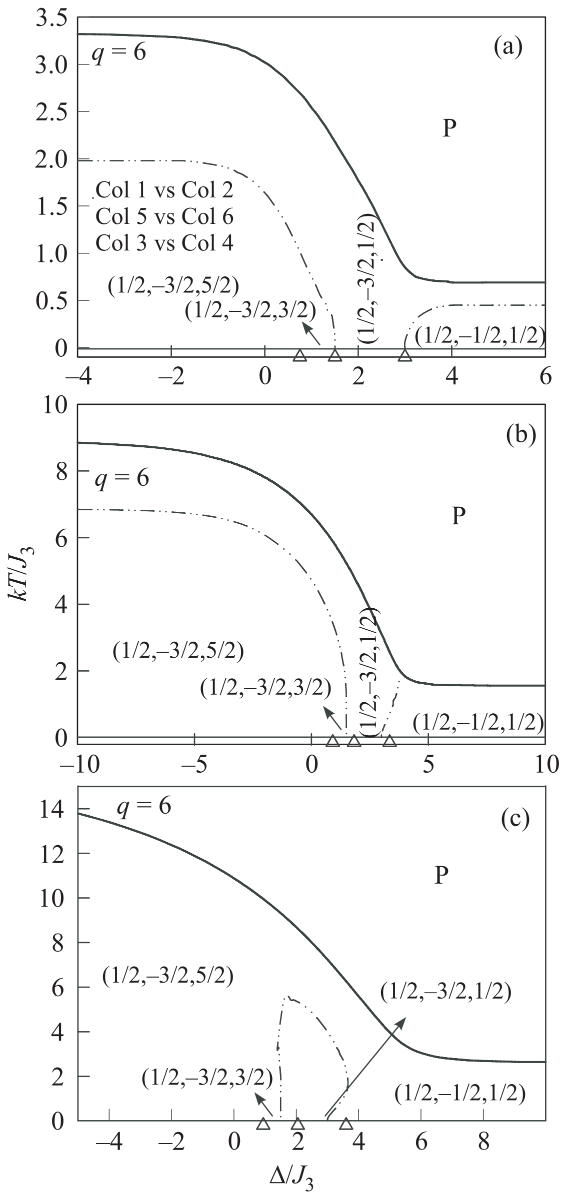

Fig.5. Phase diagrams in the $(\Delta/J_3,\ kT/J_3)$ plane for the ABC ternary system consisting of spins $\sigma = 1/2$, $S = 3/2$, and $m = 5/2$ on the Bethe lattice for the coordination number, $q = 6$. Solid line indicates a second-order phase transitions line. The filled triangles are the ordered line smoothly mediating, with no phase transition, between the (1/2, -3/2, 5/2) and (1/2, -3/2, 3/2) phases, between the (1/2, -3/2, 3/2) and (1/2, -3/2, 1/2) phases, and between the (1/2, -3/2, 1/2) and (1/2, -1/2, 1/2) phases. (a) $J_1 = -0.1$, $J_2 = -2.0$, $J_3 = 1.0$, (b) $J_1 = -1.0$, $J_2 = -2.0$, $J_3 = 1.0$, **(c)** $J_1 = -5.0$, $J_2 = -2.0$, $J_3 = 1.0$

The part of this work was supported by the Scientific and Technological Research Council of Turkey

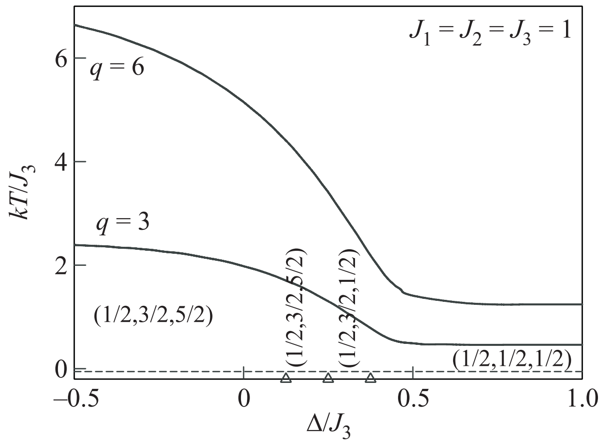

Fig.6. Same as Fig.7, but the same values of the bilinear nearest-neighbor exchange interaction parameters ($J_1 = J_3 = J_3 = 1$), $q = 6$ and $q = 3$. The filled triangles are the ordered lines smoothly mediating, with no phase transition, between the (1/2, 3/2, 5/2) and (1/2, 3/2, 5/2) phases, between the (1/2, 3/2, 5/2) and (1/2, 3/2, 1/2) phases, and between the (1/2, 3/2, 1/2) and (1/2, 1/2, 1/2) phases

(TÜBİTAK) Grant # 107T533 and Erciyes University Research Funds, Grant # FBD-08-593. One of us (B.D.) would like to express his gratitude to the (TÜBİTAK) for the Ph.D scholarship.

Appendix

The explicit expression of recursion relations are calculated as follows:

$$N_n = \frac{g_n(1/2)}{g_n(-1/2)} = \frac{\left[\begin{array}{l} e^{-\beta 9\Delta/4}\left(e^{\beta a_1} X_n^{q-1} + e^{-\beta a_1} Y_n^{q-1}\right) \\ + e^{-\beta\Delta/4}\left(e^{\beta a_1/3} Z_n^{q-1} + e^{-\beta a_1/3}\right) \end{array}\right]}{\left[\begin{array}{l} e^{-\beta 9\Delta/4}\left(e^{\beta a_2/3} X_n^{q-1} + e^{-\beta a_2} Y_n^{q-1}\right) \\ + e^{-\beta\Delta/4}\left(e^{\beta a_2/3} Z_n^{q-1} + e^{-\beta a_2/3}\right) \end{array}\right]},$$

where

$$a_1 = 3J_1/4 + 3h/2, \text{ and } a_2 = -3J_1/4 + 3h/2;$$

$$X_n = \frac{g_n(3/2)}{g_n(-1/2)} = \frac{\left[\begin{array}{l} e^{-25\beta\Delta/4}\left(e^{\beta b_1} A_n^{q-1} + e^{-\beta b_1} B_n^{q-1}\right) \\ + e^{-9\beta\Delta/4}\left(e^{3\beta b_1/5} C_n^{q-1} + e^{-3\beta b_1/5} D_n^{q-1}\right) \\ + e^{-\beta\Delta/4}\left(e^{-\beta b_1/5} E_n^{q-1} + e^{\beta b_1/5}\right) \end{array}\right]}{\left[\begin{array}{l} e^{-25\beta\Delta/4}\left(e^{-\beta b_2} A_n^{q-1} + e^{\beta b_2} B_n^{q-1}\right) \\ + e^{-9\beta\Delta/4}\left(e^{-3\beta b_2/5} C_n^{q-1} + e^{3\beta b_2/5} D_n^{q-1}\right) \\ + e^{-\beta\Delta/4}\left(e^{-\beta b_2/5} E_n^{q-1} + e^{\beta b_2/5}\right) \end{array}\right]},$$

$$Y_n = \frac{g_n(-3/2)}{g_n(-1/2)} = \frac{\left[\begin{array}{l} {}^{-25\beta\Delta/4}\left(e^{-\beta b_3} A_n^{q-1} + e^{\beta b_3} B_n^{q-1}\right) \\ + e^{-9\beta\Delta/4}\left(e^{-3\beta b_1/5} C_n^{q-1} + e^{3\beta b_1/5} D_n^{q-1}\right) \\ + e^{-\beta\Delta/4}\left(e^{-\beta b_1/5} E_n^{q-1} + e^{\beta b_1/5}\right) \end{array}\right]}{\left[\begin{array}{l} e^{-25\beta\Delta/4}\left(e^{-\beta b_2} A_n^{q-1} + e^{\beta b_2} B_n^{q-1}\right) \\ + e^{-9\beta\Delta/4}\left(e^{-3\beta b_2/5} C_n^{q-1} + e^{3\beta b_2/5} D_n^{q-1}\right) \\ + e^{-\beta\Delta/4}\left(e^{-\beta b_2/5} E_n^{q-1} + e^{\beta b_2/5}\right) \end{array}\right]},$$

$$Y_n = \frac{g_n(1/2)}{g_n(-1/2)} = \frac{\left[\begin{array}{l} e^{-25\beta\Delta/4}\left(e^{\beta b_4} A_n^{q-1} + e^{-\beta b_4} B_n^{q-1}\right) \\ + e^{-9\beta\Delta/4}\left(e^{3\beta b_4/5} C_n^{q-1} + e^{-3\beta b_4/5} D_n^{q-1}\right) \\ + e^{-\beta\Delta/4}\left(e^{-\beta b_4/5} E_n^{q-1} + e^{\beta b_4/5}\right) \end{array}\right]}{\left[\begin{array}{l} e^{-25\beta\Delta/4}\left(e^{-\beta b_2} A_n^{q-1} + e^{\beta b_2} B_n^{q-1}\right) \\ + e^{-9\beta\Delta/4}\left(e^{-3\beta b_2/5} C_n^{q-1} + e^{3\beta b_2/5} D_n^{q-1}\right) \\ + e^{-\beta\Delta/4}\left(e^{-\beta b_2/5} E_n^{q-1} + e^{\beta b_2/5}\right) \end{array}\right]},$$

where

$$b_1 = 15J_2/4 + 5h/2, \; b_2 = 5J_2/4 - 5h/2,$$
$$b_3 = 15J_2/4 - 5h/2, \text{ and } b_4 = 5J_2/4 + 5h/2;$$

$$A_n = \frac{g_n(5/2)}{g_n(-1/2)} = \frac{e^{-\beta\Delta/4}\left[e^{\beta c_1} N_{n-1}^{q-1} + e^{-\beta c_1}\right]}{e^{-\beta\Delta/4}\left[e^{\beta c_2} N_{n-1}^{q-1} + e^{-\beta c_2}\right]},$$

$$B_n = \frac{g_n(-5/2)}{g_n(1/2)} = \frac{e^{-\beta\Delta/4}\left[e^{\beta c_3} N_{n-1}^{q-1} + e^{-\beta c_3}\right]}{e^{-\beta\Delta/4}\left[e^{\beta c_2} N_{n-1}^{q-1} + e^{-\beta c_2}\right]},$$

$$C_n = \frac{g_n(3/2)}{g_n(-1/2)} = \frac{e^{-\beta\Delta/4}\left[e^{\beta c_4} N_{n-1}^{q-1} + e^{-\beta c_4}\right]}{e^{-\beta\Delta/4}\left[e^{\beta c_2} N_{n-1}^{q-1} + e^{-\beta c_2}\right]},$$

$$D_n = \frac{g_n(-3/2)}{g_n(-1/2)} = \frac{e^{-\beta\Delta/4}\left[e^{\beta c_5} N_{n-1}^{q-1} + e^{-\beta c_5}\right]}{e^{-\beta\Delta/4}\left[e^{\beta c_2} N_{n-1}^{q-1} + e^{-\beta c_2}\right]},$$

$$E_n = \frac{g_n(1/2)}{g_n(-1/2)} = \frac{e^{-\beta\Delta/4}\left[e^{\beta c_6} N_{n-1}^{q-1} + e^{-\beta c_6}\right]}{e^{-\beta\Delta/4}\left[e^{\beta c_2} N_{n-1}^{q-1} + e^{-\beta c_2}\right]},$$

where

$$c_1 = 5J_3/4 + h/2, \; c_2 = -J_3/4 + h/2,$$
$$c_3 = -5J_3/4 + h/2, \; c_4 = 3J_3/4 + h/2,$$
$$c_5 = -3J_3/4 + h/2, \text{ and } c_6 = J_3/4 + h/2.$$

1. O. Sato, T. Iyoda, A. Fujishima, and K. Hashimoto, Science **271**, 49 (1996).
2. T. Kawamoto, Y. Asai, and S. Abe, Phys. Rev. Lett. **86**, 348 (2001).
3. A. Kumar, S. M. Yusuf, and L. Keller, Phys. Rev. B **71**, 054414 (2005).
4. O. Sato, T. Iyoda, A. Fujishima, and K. Hashimoto, Science **272**, 704 (1996).
5. S. Ohkoshi, A. Fujishima, and K. Hashimoto, J. Am. Cem. Soc. **120**, 5349 (1998).
6. H. W. Liu, K. Matsuda, Z. Z. Gu, K. Takahashi et al., Phys. Rev. Lett. **90**, 167403 (2003).
7. S. Ohkoshi, T. Hozumi, and K. Hashimoto, Phys. Rev. B **64**, 132404 (2001).
8. O. Sato, S. Hayami, and Y. Einaga, Bull. Chem. Soc. Japan **76**, 443 (2003).
9. S. G. Salunke, F. Varret, I. Maurin et al., J. Phys. Chem. B **109**, 8251 (2005).
10. J.-H. Park, F. Frye, N. E. Anderson et al., J. Magn. Magn. Mater. **310**, 1458 (2007).
11. S. S. Kaye and J. R. Long, J. Am. Chem. Soc. **127**, 8590 (2005).
12. M. Mansuripur, J. Appl. Phys. **61**, 1580 (1987).
13. C. Mathoniere, C. J. Nuttall, S. G. Carling, and P. Day, Inorg. Chem. **35**, 1201 (1996).
14. S. Ohkoshi, T. Iyoda, A. Fujishima, and K. Hashimoto, Phys. Rev. B **56**, 11642 (1997).
15. S. S. Kaye and J. R. Long, J. Am. Chem. Soc. **127**, 8590 (2005).
16. E. Manuel, M. Evangelisti, M. Affronte et al., Phys. Rev. B **73** 172406 (2006).
17. M. Pregelj, A. Zorko, D. Aron et al., J. Magn. Magn. Mater. **316**, e680 (2007).
18. W. Dong, W. Zhang, Y.-O. Yang et al., J. Magn. Magn. Mater. **309**, 7 (2007).
19. A. Bobák and J. Dely, Physica A **341**, 281 (2004).
20. A. Bobák, F. O. Abubrig, and D. Horvcth, Physica A **312**, 187 (2002).
21. W. Liu, Z. Xin, and X. Wang, Phys. Lett. A **372**, 1114 (2008).
22. O. Canko, B. Deviren, and M. Keskin, JETP Lett. **87**, 633 (2008).
23. B. Deviren, O. Canko, and M. Keskin, J. Magn. Magn. Mater. **321**, 1231 (2009).
24. S. Ohkoshi and K. Hashimoto, Phys. Rev. B **60**, 12820 (1999).
25. A. Bobák, F. O. Abubrig, and T. Balcerzak, Phys. Rev. B **68**, 224405 (2003).
26. A. Bobák, J. Dely, and T. Balcerzak, Czech. J. Phys. **54**, D523 (2004).
27. A. Bobák, F. O. Abubrig, and T. Balcerzak, J. Magn. Magn. Mater. **272–276**, 989 (2004).
28. H. Hu, Z. Xin, and W. Liu, Phys. Lett. A **357**, 388 (2006).
29. G. M. Buendía and J. E. Villarroel, J. Magn. Magn. Mater. **310**, e495 (2007); E. Kış-Çam and E. Aydıner, J. Magn. Magn. Mater. **322**, 1706 (2010); M. Žukovič and A. Bobák, J. Magn. Magn. Mater, in press.
30. J. Dely and A. Bobák, J. Magn. Magn. Mater. **305**, 464 (2006).
31. A. Bobák, F. O. Abubrig, and T. Balcerzak, Physica A **326**, 151 (2003).
32. S. Tsuji, T. Kasama, and T. Idogaki, J. Magn. Magn. Mater. **310**, e471 (2007).
33. J. Dely and A. Bobák, J. Magn. Magn. Mater. **305**, 464 (2006).
34. J. Dely and A. Bobák, Physica B **388**, 49 (2007).
35. J. Dely and A. Bobák, Physica B **399**, 155(2007).
36. L. Čanová, J. Strečka, and J. Dely, arXiv:cond-mat/0612426v1
37. J. Dely, A. Bobák and M. Zukovi, Phys. Lett. A **373**, 3197 (2009).
38. C. K. Hu, N. Sh. Izmailian, and K. B. Oganesyan, Phys. Rev. E **59**, 6489 (1999).
39. H. P. D Shieh and M. H. Kryder, Appl. Phys. Lett. **49**, 473 (1986).
40. G. A. N. Connell, R. Allen, and M. Mansuripur, J. Appl. Phys. **53**, 7759 (1982).
41. J. Ostorro, M. Escorne, A. P. Gugan et al., J. Appl. Phys. **75**, 6103 (1994).
42. L. Néel and Ann. Phys. **3**, 137 (1948).
43. S. Chikazumi, *Physics of Ferromagnetism*, Oxford University Press, Oxford, 1997.
44. B. Renklioğlu, A. N. Berker, and M. Keskin, Phys. Rev. Lett., to be submitted.
45. B. Deviren, M. Keskin, and O. Canko, Physica A **388**, 1835 (2009).